A native mass spectrometry platform identifies HOP inhibitors that modulate the HSP90–HOP protein–protein interaction

COMMUNICATION

A Native Mass Spectrometry Platform Identifies HOP Inhibitors that modulate the HSP90 – HOP Protein-Protein Interaction

Received 00th January 20xx,
Accepted 00th January 20xx

DOI: 10.1039/x0xx00000x

Clinton G. L. Veale,*[a] Maria Mateos-Jiménez,[b] Michaelone C. Vaaltyn,[c] Ronel Müller,[a] Matodzi P. Makhubu,[c] Mahama Alhassan,[a] Beatriz G. de la Torre,[d] Fernando Albericio,[a] C. Logan Mackay,[b] Adrienne L. Edkins[c] and David J. Clarke*[b]

Herein we describe a native mass spectromery protein-peptide model as a competent surrogate for the HOP–HSP90 Protein-Protein Interaction (PPI), application of which led to the qualititive identification of two new peptides capable of *in vitro* PPI disruption. This proof of coencept study offers a viable alternative for PPI inhibitor screening.

Traditional approaches to drug discovery have sought to disrupt critical biological processes through the direct inhibition of a well-defined subset of protein targets.[1] However the majority of these protein targets, and their ensuing biological functions, are governed by highly specific interfacial associations between partner proteins. Targeting these Protein-Protein Interactions (PPIs) offers the opportunity to expand the volume of druggable chemical space, beyond the current tried and tested model.[2] The most commonly cited challenge in identifying inhibitors of PPIs is the lack of molecular topography inherent to protein interfaces, which reduces opportunities for ligand binding.[3] However, the development of robust assay platforms from which to identify PPI inhibitors, where difficulties in differentiating between genuine binding molecules and artefacts, as well as the relatively high false positive rates of fluorescent methodologies as a result of fluorescent or redox active small molecules, remains a substantial additional challenge.[4] Therefore, the development of orthogonally operating methodologies, which can measure changes to the binding affinity between two full-length proteins or between a full-length protein and a truncated peptide, acting as a protein-proxy, is required for the validation or indeed the identification of high quality hit PPI inhibitors. To this end, several common biophysical techniques including X-ray crystallography, nuclear magnetic resonance (NMR) spectroscopy, differential scanning fluorimetry, surface plasmon resonance and isothermal titration calorimetry, as well as non-native mass spectrometry based techniques have been employed in the development of PPI drug discovery platforms.[5] However, it is common for these methods to suffer from relatively low throughput in addition to large sample consumption and extensive experimental set-up.[6]

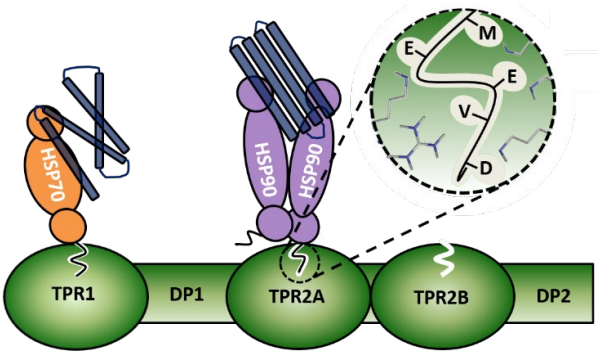

Fig.1. Schematic representation of the HSP70-HOP-HSP90 ternary chaperone complex, which mediates client protein folding. The highlighted region, representing the interface of interest in this study, is controlled by the interaction of the acid rich HSP90 *C*-terminal MEEVD motif and the positively charged carboxylate clamp of the TPR2A domain of HOP.

Conversely, native mass spectrometry (MS) provides a comparatively fast and extremely sensitive method for the analysis and direct monitoring of relatively weak non-covalent interactions of label-free protein assemblies and protein-ligand interactions in the gas phase.[7] In addition, native MS analysis allows for the rapid evaluation of relative binding affinity and approximate dissociation constants, in addition to quantitative determination of binding stoichiometry of intact complexes and protein-ligand interactions.[8] Furthermore, the orthogonal use of ion-mobility (IM), provides insight into conformation, structure, and complex stability,[9] which traditionally, could only

[a] *FLAIR Research Fellow, School of Chemistry and Physics, Pietermaritzburg Campus, University of KwaZulu-Natal, Private Bag X01, Scottsville, 3209, South Africa.*
[b] *EaStCHEM School of Chemistry, University of Edinburgh, Joseph Black Building, David Brewster Road, Edinburgh EH93FJ, UK*
[c] *The Biomedical Biotechnology Research Unit (BioBRU), Department of Biochemistry and Microbiology, Rhodes University, Makhanda, South Africa.*
[d] *KwaZulu-Natal Research Innovation and Sequencing Platform (KRISP), School of Laboratory Medicine and Medical Sciences, College of Health Sciences, University of KwaZulu-Natal, South Africa.*
† *E-mail corresponding author: VealeC@ukzn.ac.za, dave.clarke@ed.ac.uk*
Electronic Supplementary Information (ESI) available in the online version. See DOI: 10.1039/x0xx00000x

be observed through ^{15}N labelled NMR experiments and X-ray co-crystallography.[10] However, despite these advantages, very few native MS based platforms for the identification of PPI inhibitors have been described.[11]

Given that PPIs offer an innovative means of inhibiting challenging drug targets, we turned our attention to Heat Shock Protein (HSP) 90. Despite their initial promise, traditionally derived *N*-terminal ATP antagonists of HSP90 are associated with numerous limitations, preventing their clinical development.[12] As such, disruption of the PPI between HSP90 and its *C*-terminal associating co-chaperones have been highlighted as viable targets to expand the HSP90 inhibition toolbox.[13] One such co-chaperone HSP70-HSP90 organising protein (HOP), binds simultaneously to HSP70 and HSP90, and facilitates the transfer of partially folded client proteins thus mediating appropriate protein folding (**Fig.1**). Inhibition of this PPI, indirectly disrupts HSP90 mediated protein folding, without stimulating the compensatory transcriptional upregulation of HSP70, and is considered a promising target for cancer chemotherapy.[14] In addition, recent evidence suggests that the HSP70-HOP-HSP90 ternary complex is required for proteasome assembly and efficient proteasomal-mediated protein turnover.[15] The PPI interaction between HSP90 and HOP is mediated primarily by a series of salt bridges between a *C*-terminal MEEVD pentapeptide motif of HSP90 and the carboxylate clamp region of the tetratricopeptide repeat 2A (TPR2A) domain of HOP.[16] McAlpine and co-workers have recently reported the design of cyclic peptides which disrupt this PPI through binding to the MEEVD region of HSP90.[17] We reasoned that an alternative means of disrupting the HOP-HSP90 interaction might be through identifying ligands which bind directly to HOP, an idea which has been explored by Regan and co-workers.[18]

Through a comprehensive study utilising acetylated analogues of MEEVD, Brinker et al. identified the interaction between the TPR2A domain of HOP and the MEEVD peptide as the fundamental contact for HOP-HSP90 association[19] and as such represented a suitable proxy for studying the PPI.[20] Further structural insight into this interaction was provided by an X-ray co-crystal between Ac-MEEVD-OH (**1, Fig. 2**) and TRP2A.[21]

Given the importance of this specific interaction to the final formation of the HOP-HSP90 PPI, we reasoned that it could prove a useful system to assess native IM-MS as a tool for developing competent PPI models, suitable for use as PPI drug discovery platforms. Native MS solution conditions and sample infusion by an automated nano-electrospray robot allows for rapid chromatography-free data acquisition (20-60 seconds), suitable for sampling from multiwell plate formats (see supporting information). Using this system, native MS analysis of a 1:1 solution of TPR2A and **1**, showed the formation of our desired interaction at an observed binding ratio of approximately 1:0.7 (**Fig. 3A and B**). IM analysis of the $[M+8H]^{8+}$ ion of apo-TPR2A and the TPR2A–**1** complex revealed similar arrival time distributions consisting of a major compact gas phase conformation (**Fig. S1A**). The calculated collisional cross section (CCS) values of TPR2A (1603.55 ± 161.1) and the TPR2A – **1** complex (1630.62 ± 151.7) were in close agreement with the theoretical values determined by analysis of the available structures of apo-TPR2A (1655.75 ± 12.02, PDB 2NC9) and the TPR2A-**1** complex (1662.1, PDB 1ELR, **Fig. S1B**).

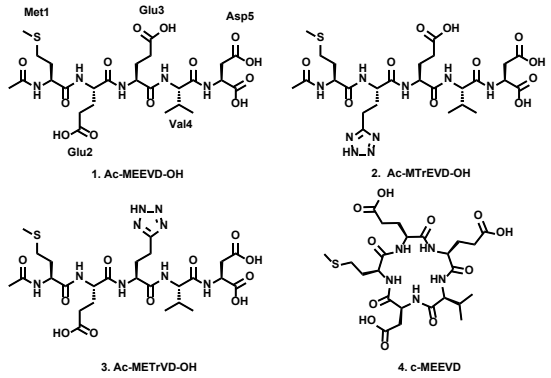

Fig. 2. Pentapeptides used in this study.

These data provided good evidence that the solution phase structure of the apo and ligand bound species was retained into the gas phase during native nESI ionisation, which is a key factor when attempting to identify genuine binding ligands. Given the potential of tetrazoles as acid bioisosteres in drug discovery,[22] we synthesized two Ac-MEEVD-OH analogues, Ac-MTrEVD-OH (**2**) and AcMETrVD-OH (**3, Fig.2**), in which one of the glutamic acid residues were substituted with the corresponding tetrazole containing non-canonical amino acid. Furthermore, based on the success of McAlpine's cyclic peptides, we reasoned that a cyclic MEEVD analogue may provide useful insight.[17] Native MS analysis of TPR2A preincubated with either **2** (**Fig. S2**), **3** (**Fig. S3**) or **4** at a 1:1 stoichiometry revealed that both the tetrazole containing peptides bound to TPR2A with a similar affinity as that observed for **1**, while binding was not detected for **4**. Native mass spectra obtained from a 1:1:1 buffered solution of TPR2A–**1** co-incubated with either peptide **2** or **3** again produced the apo TPR2A and **1** bound species in addition to the species corresponding to the binding of peptide **2** or **3** (**Fig. 4A and B**).

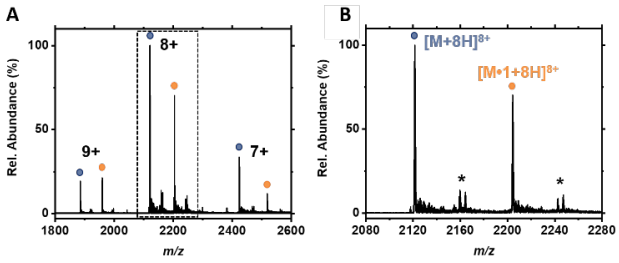

Fig. 3. A. Native mass spectrum of the 1:1 buffered solution of TPR2A and **1**. **B.** Expanded region of the 8^+ charge state, showing the apo TPR2A (blue, *m/z* 2121.5, $[M+8H]^{8+}$) and the TPR2A-**1** complex (orange, *m/z* 2204.4, $[M•1+8H]^{8+}$). *protein impurities derived from protease cleavage during His-TPR2A purification.

No evidence of a ternary complex, i.e. simultaneous peptide binding was observed, suggesting that these peptides bind at the same site, in a competitive manner. The abundance ratios of each species indicated that in comparison to **1**, both tetrazole containing peptides preferentially bound to TPR2A, resulting in partial disruption of the TPR2A:MEEVD interface. Ratiometric analysis of the signals corresponding to the three species

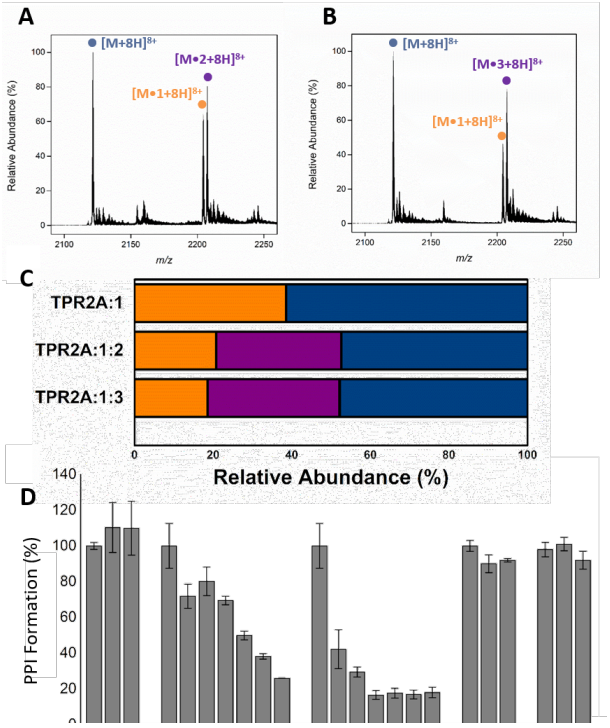

Fig. 4: Expanded region of the 8^+ charge state, of the 1:1:1 buffered mixture of TPR2A, **1** and **2** (**A**) or **3** (**B**) showing apo TPR2A (blue) the TPR2A – **1** complex (orange) and the TPR2A – **2** or TPR2A – **3** complexes (purple, *m/z* 2207.5 $[M+H]^{8+}$). **C:** Ratiometric analysis of the MS apo (blue), the TPR2A – **1** complex (orange) the TPR2A – **2** or TPR2A – **3** complexes (purple), in the absence of (top) and presence of peptides **2** and **3** suggesting that these peptides inhibit AcMEEVD-OH binding. **D:** Solid phase PPI ELISA assay, between the HOP TRP2A domain and the HSP90 *C*-terminal domain. Peptides **2** (pIC_{50} 5.1) and **3** (pIC_{50} 6.5) both disrupted the PPI in a dose dependant manner, while **1** and **4** were inactive.

observed in the mass spectra (**Fig. 4C**), revealed that in the absence of peptides **2** and **3** the relative abundance of apo TPR2A to TPR2A–**1** existed at a ratio of 61%:39% (**Table S1**). Introduction of peptide **2** and subsequent binding to TPR2A unsurprisingly reduced the relative abundance of apo TPR2A to 47%, but had a far more pronounced effect on the TPR2A–**1** species, reducing this to 21%. Similarly, peptide **3** was found to reduce apo-TPR2A abundance to 48%, with the TPR2A–**1** species decreased to 19%, representing a 49% change in the abundance of TPR2A-**1**, thus strongly indicating that binding of peptides **2** and **3** to TPR2A occurred via displacement of peptide **1**. In order to determine whether the disruption of **1** provided a competent model of PPI disruption, peptides **1 – 4** were assayed for PPI inhibition in an ELISA-based PPI solid phase assay (**Fig. 4D**).[23] Peptide **1**, has traditionally been associated with weak disruption of the HOP-HSP90 PPI,[19] however at our experimental concentration range, **1** was incapable of disrupting the target PPI. Similarly, peptide **4** whose binding was not detectable in our set-up, was also inactive. Conversely, peptides **2** and **3** were found to disrupt the PPI between the TPR2A and the HSP90 *C*-terminal in a dose-dependent manner. Incidentally, while the ratiometric analysis indicated that peptide **3**, was slightly more efficient than **2** at disrupting Ac-MEEVD-OH binding, in the solid phase assay, peptide **3**, was found to be an order of magnitude more effective than peptide **2** at disrupting the target PPI. This therefore suggests that our model is useful for the qualitative indication of PPI inhibitory potential but falls short in quantification of this effect.

Finally, for structural insight into the observed activity, we conducted an *in silico* assessment of our inhibitory peptides using the X-ray co-crystal structure or the TRR2A–**1** complex (PDB 1ELR).[21] In line with a previous in-depth *in silico* study,[20] redocking of **1**, followed by molecular mechanics minimisation, placed the ligand in a similar binding mode to that solved for the co-crystal. Here in addition to the Val4 residue of peptide **1** occupying a prominent hydrophobic pocket, the Met1 residue (Lys239), the side chain residue of Glu2 (Asn308, Arg305), the backbone carbonyl of Glu3 (Arg305), and both the terminal (Lys229, Asn233, Asn264) and side chain residue (Lys301, Gln298) of Asp5 formed a series of electrostatic interactions along the binding grove of TPR2A.

Curiously, however the side chain residue of Glu3 was not found to participate in any electrostatic interactions (**Fig. 5A**). The highest scoring docking pose of peptide **3** showed that in contrast to the crystal structure, the bioisosteric tetrazole moiety interacted with Lys237. The preferential formation of this interaction resulted in the ligand shifting position within the binding groove slightly, sacrificing its interaction with Asn308, whilst maintaining electrostatic interactions with the remaining residues as **1**, albeit at different orientations (**Fig. 5B**). *In silico* assessment of peptide **2** showed that the tetrazole occupied a similar region to the corresponding Glu2 of peptide **1**, thus reforming the interaction with Asn308. While, the VD region of peptide **2** was predicted to occupy a different region of the binding groove, these data also suggested that Glu3 interacted with Lys237, albeit to a lesser extent that peptide **3** (**Fig. S4**). In addition to Lys238 and 239, Lys237 has been suggested to be a key residue for selective HOP-HSP90 interaction.[24,25]

Therefore, the capacity of peptides **2** and **3**, to directly interact with this residue, with **1** seemingly less able to do so, may account for the peptide binding and PPI inhibitory activity of the tetrazole containing peptides.

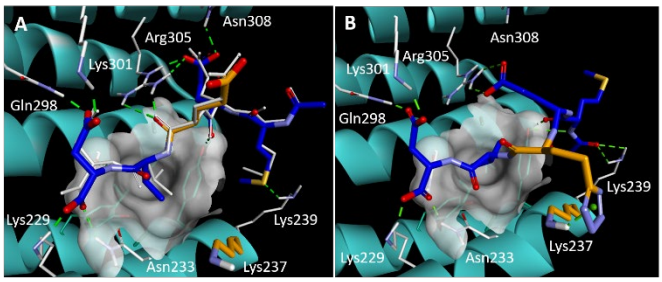

Fig.5A: Co-crystallised (white) and re-docked (blue/orange) binding pose of peptide **1** (RMSD 0.261), in the HSP90 recognition groove of the HOP-TPR2A domain (1ELR). White surface depicts the hydrophobic pocket. Glu3 and Lys 237 (orange) do not interact. **B:** Lowest energy docked pose of peptide **3**, indicating the formation of an electrostatic interaction between Lys237 and the tetrazole moiety, providing a structural basis for Ac-MEEVD-OH binding inhibition and PPI inhibition.

To conclude, for the efficient exploitation of PPIs as tractable targets in drug discovery, the development of reliable orthogonal methods to identify or validate hit compounds is vital. We present here a proof of principle study demonstrating the potential of native MS based platforms to study models of

PPIs based on protein-peptide surrogates. Our methodology allowed us to structurally examine our protein-peptide model in order to identify peptide-based inhibitors. Two rationally designed tetrazole containing peptides were found to disrupt the PPI model, which importantly, translated into *in vitro* PPI inhibition. Several powerful methodologies, such as phage display, have been developed to identify high-affinity peptide binders.[26] However, while often successfully used to identify PPI inhibitors, these approaches select for peptide binding and are not by default tuned to identify PPI inhibitors. Conversely, this study focussed on simultaneously identifying genuine binders and detecting potential PPI disruptors without the need for isotope labelling, tethering, or ligand assay interference. However, it is important to note that while the MS methodology was capable of quantifying binding stoichiometry, it appears that rapid screening would not be quantitative. The scope of this study was limited to a well-characterised protein-peptide interaction, leading to the identification of two new PPI inhibitory peptides, demonstrating that native MS PPI models are capable of identifying PPI inhibitors. Therefore, given the inherent advantages of native MS with respect to speed, sensitivity, and relativity simple experimental set up, this approach provides a useful additional complimentary strategy to qualitatively screen for quality PPI inhibitory peptides or non-peptide small molecules. Based on the inhibitory data obtained here, and the potential of this target, we are currently conducting an in-depth medicinal chemistry study into the structural parameters required for selective PPI inhibition, with a view to further elucidating the role of this PPI in cancer pathogenesis and developing new therapies for difficult to treat cancers.

Notes and references

The authors acknowledge support from the National Research Foundation of South Africa (NRF, Grant No. 116305, 105829 and 127224), the South African Research Chairs Initiative of the Department of Science and Innovation (DSI) and NRF (Grant No. 98566), the Royal Society-Newton Fund (Grant No. NI160018), the BBSRC (Grant No. BB/R013993/1), Rhodes University, the University of KwaZulu-Natal Flagship Initiative and Future Leaders – African Independent Research (FLAIR), a partnership between the African Academy of Sciences and the Royal Society that is funded by the UK Government as part of the Global Challenge Research Fund (GCRF). RM, MCV and MPM gratefully acknowledge support from the NRF. We thank the Centre for High Performance Computing (CHPC) for access to Schrodinger's modelling suite and Prof. Lynne Regan for the kind gift of the expression plasmid for TPR2A.

1 S. C. Bull and A. J. Doig, *PLoS One*, 2015, **10**, e0117955.
2 B. O. Villoutreix, C. M. Labbe, D. Lagorce, G. Laconde and O. Sperandio, *Curr. Pharm. Des.*, 2012, **18**, 4648–4667.
3 S. Surade and T. L. Blundell, *Chem. Biol.*, 2012, **19**, 42–50.
4 J. B. Baell and J. W. M. Nissink, *ACS Chem. Biol.*, 2018, **13**, 36–44.
5 A. Dailing, A. Luchini and L. Liotta, *Expert Rev. Proteomics*, 2015, **12**, 457–467.
6 X. Chen, S. Qin, S. Chen, J. Li, L. Li, Z. Wang, Q. Wang, J. Lin, C. Yang and W. Shui, *Sci. Rep.*, 2015, **5**, 8361.
7 L. A. Woods, O. Dolezal, B. Ren, J. H. Ryan, T. S. Peat and S.-A. Poulsen, *J. Med. Chem.*, 2016, **59**, 2192–2204.
8 J. T. S. Hopper and C. V. Robinson, in *Proteomics for Biological Discovery*, John Wiley & Sons, Inc., Hoboken, NJ, USA, 2019, pp. 145–173.
9 C. G. L. Veale, M. Mateos Jimenez, C. L. L. Mackay and D. J. D. J. Clarke, *Rapid Commun. Mass Spectrom.*, 2020, **34**, e8570.
10 J. Stojko, S. Fieulaine, S. Petiot-Bécard, A. Van Dorsselaer, T. Meinnel, C. Giglione and S. Cianférani, *Analyst*, 2015, **140**, 7234–7245.
11 D. Cubrilovic, K. Barylyuk, D. Hofmann, M. J. Walczak, M. Gräber, T. Berg, G. Wider and R. Zenobi, *Chem. Sci.*, 2014, **5**, 2794–2803.
12 L. Wang, L. Zhang, L. Li, J. Jiang, Z. Zheng, J. Shang, C. Wang, W. Chen, Q. Bao, X. Xu, Z. Jiang, J. Zhang and Q. You, *Sci. Adv.*, 2019, **5**, 2277.
13 A. L. Edkins, *Top. Med. Chem.*, 2016, **19**, 21–54.
14 A. L. Cortajarena, F. Yi and L. Regan, *ACS Chem. Biol.*, 2008, **3**, 161–166.
15 K. Bhattacharya, L. Weidenauer, T. M. Luengo, E. C. Pieters, P. C. Echeverría, L. Bernasconi, D. Wider, Y. Sadian, M. B. Koopman, M. Villemin, C. Bauer, S. G. D. Rüdiger, M. Quadroni and D. Picard, *Nat. Commun.*, 2020, **11**, 5975.
16 S. C. Onuoha, E. T. Coulstock, J. G. Grossmann and S. E. Jackson, *J. Mol. Biol.*, 2008, **379**, 732–744.
17 M. N. Rahimi and S. R. McAlpine, *Chem. Commun.*, 2019, **55**, 846–849.
18 G. Pimienta, K. M. Herbert and L. Regan, *Mol. Pharm.*, 2011, **8**, 2252–2261.
19 A. Brinker, C. Scheufler, F. Von Der Mülbe, B. Fleckenstein, C. Herrmann, G. Jung, I. Moarefi and F. Ulrich Hartl, *J. Biol. Chem.*, 2002, **277**, 19265–19275.
20 M. Lapelosa, *J. Chem. Theory Comput.*, 2017, **13**, 4514–4523.
21 C. Scheufler, A. Brinker, G. Bourenkov, S. Pegoraro, L. Moroder, H. Bartunik, F. U. Hartl and I. Moarefi, *Cell*, 2000, **101**, 199–210.
22 F. Allen, J. W. Liebeschuetz, C. Groom, D. A. Bardwell, T. S. G. Olsson and P. A. Wood, *J. Chem. Inf. Model.*, 2012, **52**, 857–866.
23 M. C. Hunter, K. L. O'Hagan, A. Kenyon, K. C. H. Dhanani, E. Prinsloo and A. L. Edkins, *PLoS One*, 2014, **9**, e86842.
24 S. Daniel, G. Bradley, V. M. Longshaw, C. Söti, P. Csermely and G. L. Blatch, *Biochim. Biophys. Acta - Mol. Cell Res.*, 2008, **1783**, 1003–1014.
25 P. Muller, E. Ruckova, P. Halada, P. J. Coates, R. Hrstka, D. P. Lane and B. Vojtesek, *Oncogene*, 2013, **32**, 3101–3110.
26 A. J. Quartararo, Z. P. Gates, B. A. Somsen, N. Hartrampf, X. Ye, A. Shimada, Y. Kajihara, C. Ottmann and B. L. Pentelute, *Nat. Commun.*, 2020, **11**, 3183.

